Model-Based Approach to Tomographic Reconstruction Including Projection Deblurring. Sensitivity of Parameter Model to Noise on Data

Jean Michel Lagrange[1] and Isabelle Abraham[1]

Commissariat à l'Energie Atomique, B.P. 12
91680 Bruyères le Chatel, France
{jean-michel.lagrange,isabelle.abraham}@cea.fr

Abstract. Classical techniques for the reconstruction of axisymmetrical objects are all creating artefacts (smooth or unstable solutions). Moreover, the extraction of *very* precise features related to big density transitions remains quite delicate. In this paper, we develop a new approach -in one dimension for the moment- that allows us both to reconstruct and to extract characteristics: an a priori is provided thanks to a density model. We show the interest of this method in regard to noise effects quantification ; we also explain how to take into account some physical perturbations occuring with real data acquisition.

Keywords: tomography, flexible models, regularization, deblurring.

1 Introduction

From the last ten years, teams of researchers have worked on tomographic reconstruction of objects from a very little number of views ; the final goal being to delimit very precisely big transitions of density between the various materials [15,8,20,19,23,9] (typically in angiography) and also to restitute good values of the density field when the objects are not binary.

The general context of our study is the reconstruction, from a single X-ray photograph, of an object with a symmetry of revolution ; here, we assume that X-rays are parallel (because the objects are sufficiently far from the emitter) and monoenergetic. This work is part of a hydrodynamic high yield test project where we study the dynamic behaviour of objects constrained by shock waves produced with explosives. Due to the very hostile experimental environment, there is only a single X-ray machine. So as to make out the signals received on detectors, we have to research, from the unique projection, the interfaces between the different areas of the object in order to labellize a posteriori the materials. Moreover, it is fundamental, for us, to estimate precisely their respective masses: this operation implies a very good knowlegde of the density field $\rho : \mathbb{R}^3 \longrightarrow \mathbb{R}$.

T. Pajdla and J. Matas (Eds.): ECCV 2004, LNCS 3024, pp. 37–49, 2004.

The data we get in our experiences are formed in the following way:

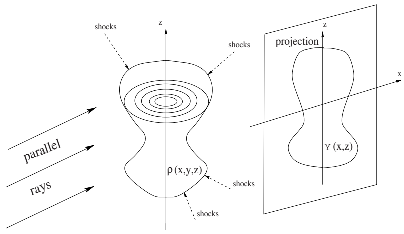

The attenuations of the X-ray beam are given by

$$att(x,z) = e^{-\int_l \frac{\mu}{\rho}(x,y,z)\rho(x,y,z)dl}$$

where $\frac{\mu}{\rho}(x,y,z)$ is the attenuation coefficient at the point (x,y,z). As source illumination is monoenergetic, we can define a reference attenuation coefficient $(\frac{\mu}{\rho})_{ref}$, constant everywhere in the spatial domain. This allows us to write:

$$att(x,z) = e^{-(\frac{\mu}{\rho})_{ref}\int_l \frac{\frac{\mu}{\rho}(x,y,z)}{(\frac{\mu}{\rho})_{ref}}\rho(x,y,z)dl} = e^{-(\frac{\mu}{\rho})_{ref}\int_l \rho_{ref}(x,y,z)dl}$$

where ρ_{ref} is the equivalent density of the reference material. The quantity

$$\mathcal{Y}(x,z) = \int_l \rho_{ref}(x,y,z)dl \tag{1}$$

is defined as the projection of the equivalent object.

Remark 1. *If ρ_{ref} is known at each point (x,y,z) and if the materials are labellized (very often thanks to expert analysis) then $\frac{\mu}{\rho}(x,y,z)$ is known and the whole density field can be obtained using the following conversion:*

$$\rho(x,y,z) = \rho_{ref}(x,y,z) \times \frac{(\frac{\mu}{\rho})_{ref}}{\frac{\mu}{\rho}(x,y,z)} \tag{2}$$

The datas $\mathcal{Y}$ of the reconstruction processes are biased by the systems of production and acquisition of X-ray photons. The two main perturbations are the **additive noise on the projections** and the presence of **blur** due to the X source and the detector (see [18] for more details).

Under these hypotheses, tomographic reconstruction of axisymmetrical objects from a single projection is technically achievable [1] (thanks to axisymmetry) but it remains very delicate: generally, this leads to an inverse problem which is well known to be ill-posed in the sense of Hadamard [13] because the solution sensitivity (to noise) is very high.

Historically, in this context, Abel proposed in 1826 [1] a method based on the inversion of his tranform [3]. This approach has been improved more recently [5] [14] [11] so as to decrease the artefacts generated by noise on projections. However, the results remain again too unstable.

Some authors [14] [10] [16] proposed also to adapt classical techniques used in "conventional" tomography (Fourier synthesis and filtered backprojection): the idea is to duplicate the unique projection to simulate acquisition from a large number of angles. All these reconstructions have in common to create loss of resolution while correlating noise leading to difficult segmentations.

Thanks to an optimal meshing technique described in [7], it is also possible to get, for each plane section of the object, a reconstruction by *Generalized Inversion* based on a natural sampling in torus:

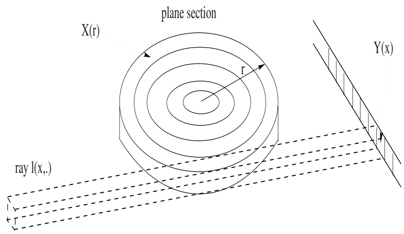

with $Y(x) = \mathcal{Y}(x, .)$ and $X(r) = X(\sqrt{x^2 + y^2}) = \rho_{ref}(x, y, .)$. On each section, we have a relation between Y and X given by $Y = HX$, where H is the projection matrix which is upper triangular and well conditionned. The solution is then simple and easy to compute as it consists in matrix inversion and multiplication, but it is very unstable: the noise is amplified, merely near the axis of symmetry [7].

The poor quality of the estimated density field lead to the introduction of regularization processes. The very easy Tikhonov-based approaches [24] are not efficient enough here because the solution is too smooth. Jean Marc Dinten [7] used Random Markov Fields (in the definition of a priori energy in a MAP criterium) allowing to decrease noise influence while preserving high density transitions. His method is indeed efficient but their remain a lot of parameters whose regulation is not straightforward.

The common characteristic of all the previous approaches is that they provide an equivalent density field ρ_{ref} which is not segmented in materials. So they necessit a supplementary process of labellization obtained after contour extraction and expert analysis in order to correct the density thanks to equation 2. The consequence is that additional uncertainties, inherent to the contour extractor, are added on the final field ρ.

Moreover, the blur present on attenuations (see section 4) is not taken into account (direct deblurring being not satisfactory) during the reconstruction process. The main effect, as shown in section 4, is to modify the estimated masses for all the materials.

In this paper, we propose a new approach where we introduce an a priori on the shape of the objects: an axisymmetrical density model. First, we treat a 1D technique where each plane section is processed in an independent way. In our experiences of high yield hydrodynamic, the shock wave propagation and multiple reflexion phenomena generate areas with approximatively linear varying

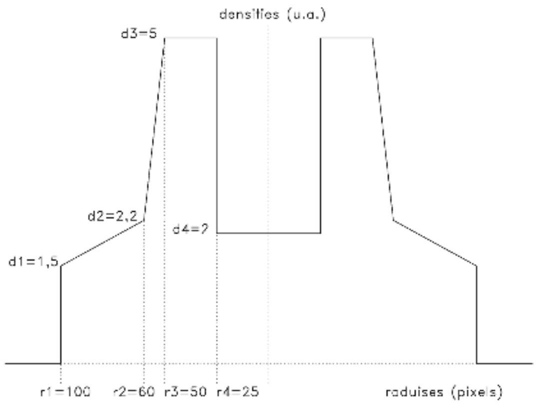

Fig. 1. Example of 1D density model

densities. (which is confirmed by physicists expert analysis), so a 1D realistic model, illustrated on figure 1, is built by juxtaposition of constant density areas and of linear varying density areas.

In section 2, we detail this approach by fitting of model. In section 3, we present a sensitivity study of the parameters of the deformable model in the case where the data are noisy. This is compared with the uncertainties obtained when we use the results of generalized inversion (that will be our reference method in this paper). In section 4, an original way to achieve deblurring/reconstruction from blurred data is exposed.

2 1D Reconstruction

We have presented, formerly, "classical techniques" for the reconstruction of a plane section of an object in equivalent densities. We also have mentionned the necessity to labellize the materials so as to correct their density.

We propose here a new approach that allows both to reconstruct and to extract the searched characteristics of the objects (radiuses of interfaces r_i and densities d_j as illustrated on figure 1) thanks to the introduction of an important a priori on the density. If we denote $\omega \in \mathbb{R}^n$ (where n is the number of parameters of the 1D model) the vector of radiuses r_i and of densities d_j, x the pixels' abscissa, $Y(x)$ the data (areal masses) and $proj_\omega(x)$ the projection model, the problem of reconstruction can be stated as follow:

$$(\mathcal{P}) \begin{cases} \widetilde{\omega} & = \arg\min_{\omega\in\Omega} \|proj_\omega - Y\|_2^2 = \arg\min_{\omega\in\Omega}(\varepsilon^2) \\ (\mathcal{C}) & : \quad \theta(\omega) \geq 0, \\ \Omega & = \quad \{\omega \in \mathbb{R}^n \ / \ \omega_l \leq \omega \leq \omega_u\} \end{cases} \tag{3}$$

where $\widetilde{\omega}$ is the solution $(\mathcal{P})$ that minimizes ε^2 ; The constraints $(\mathcal{C})$ are used to limit the domain and to ensure the existence of all the areas during the process (it's to say $r_i > r_{i+1}, \forall i$). We can notice here that the criteria ε^2 is defined continuously on Ω and performs a **sub-pixel reconstruction**.

The analysis of minimization methods (simulated annealing [12], I.C.M. [2] and gradient descents [4] [22] [21]), leads us to choose gradient descents under inequality contraints because they are faster and easier to compute with constraints (Lagrange multiplier theory) ; they also preserve the continuous aspect of the criteria.

The main problem is that $proj_\omega$, and consequently ε^2, are C^1 almost everywhere on Ω but on a finite number of points: we can show that ε^2 is infinitely differentiable with respect to the d_i and differentiable with respect to the r_i everywhere but on $r_i = |x|$, where x are the discrete positions of the data. So as to get C^1 class on Ω, we have proposed two kinds of regularizations.

Remark 2. *We will denote $A \underset{\omega}{\star} B$ the convolution of A and B in Ω and $A \underset{x}{\star} B$ the result of a spatial convolution.*

2.1 Regularization by Convolution

The main idea is to find a function $\boldsymbol{h} : I\!R^n \longrightarrow I\!R^n$, C^1 class on Ω, such that $\left[proj_\omega \underset{\omega}{\star} \boldsymbol{h}\right]$ is C^1 on Ω. So, the new criteria defined by

$$\varepsilon^2 = \left\| \left[proj_\omega \underset{\omega}{\star} \boldsymbol{h}\right] - Y \right\|_2^2 \tag{4}$$

will have the desired property. An analysis of $\left[proj_\omega \underset{\omega}{\star} \boldsymbol{h}\right]$ provides us a simple expression for $\boldsymbol{h}$:

$$\boldsymbol{h}(\omega) = \prod_{i=1}^{n_r} h_{1D}(r_i) \tag{5}$$

where n_r is the number of interface radiuses and h_{1D} a kernel defined on $I\!R$.

The kernel h_{1D} can then be expressed in the following way:

$$h_{1D}(r) = \frac{1}{\beta} \times f\left(\frac{r-x}{\beta}\right) \text{ if } x \in [r-\beta, r+\beta] \tag{6}$$

(β is the regularization parameter), where f is a gaussian like function whose support is $[-1, 1]$.

This technique proved to be efficient as we have obtained the convergence of the process of minimization of the energy given by equation 4 (for $\beta > 1$ numerically). But, as expected, the final solution depends sometimes severely on the choice of the regularization parameter β.

2.2 Regularization with a Weighting Function

In the previous subsection, we provide a way to solve our minimization problem. Unfortunately, we found that the final estimate of ω was unacceptably dependent on the regularization parameter β. Here, we propose a new manner to regularize that is simpler and quite "transparent" (i.e. independent of regularization parameters).

Let $\boldsymbol{u} : I\!R \times \Omega \longrightarrow I\!R$ be a function of class $C^p, p \geq 1$, that equals zero in a neighbourhood of all the singular points r_i, then the criteria:

$$\varepsilon^2 = \sum_{x \in \mathcal{D}} \left\{ \boldsymbol{u}(x,\omega) \Big(proj_\omega(x) - Y(x) \Big)^2 \right\}, \tag{7}$$

where $\mathcal{D}$ is the set of measure points, is C^p class on Ω.

The function $\boldsymbol{u}$ can be chosen as follow:

$$\boldsymbol{u}(x,\omega) = \prod_{i=1}^{n_r} u(x, r_i) \tag{8}$$

where $u(x,0)$ is an even function, equaling 0 in $[0,\epsilon]$ and 1 in $[k\epsilon, +\infty[$. Its graph (and the one of its first and second derivative with respect to r) is given by:

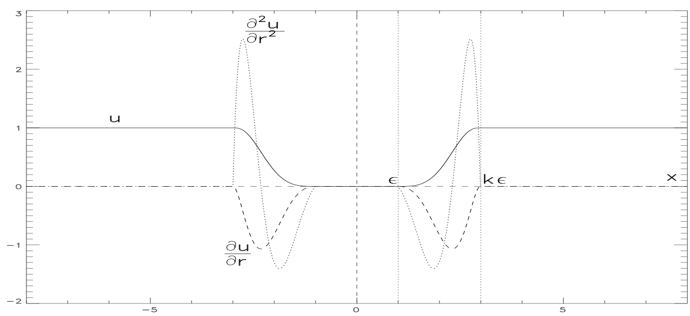

This approach, much more faster than the previous, allowed us to solve our minimization problem. Moreover, it appears that the final solution is quite independent of the choice of ϵ and k that we fix respectively at 1 and 3.

However, before reconstructing the object by 1D fitting, we must calculate the optimal number of linear varying density areas. If we denote $\widetilde{\sigma^2}$ an estimate of the noise variance, we demonstrated that this is number is correct if the optimal value of the criteria $\varepsilon^2(\widetilde{\omega})$ is close enough to $\widetilde{\sigma^2}$ and if the sensitivity (to noise present on the projections) of the parameter ω (whose expression is given in the next section) is small. For our objects, a model with eight parameters and two linear-varying areas (see figure 1) is always optimal.

3 Sensitivity to Noise

Getting a good precision on the position of the interfaces is very important in our context. If the function $\boldsymbol{u}$ defined in 2.2 is built to be C^2 class on $I\!R \times I\!R^n$, then the criteria given by equation 7 is C^2 on Ω. The zero-crossing condition of the gradient of ε^2 in an acceptable openset leads to an implicit system $F(\omega, Y) = 0$ where F is continuously differentiable and has an inversible jacobian matrix. Under these conditions, the implicit functions theorem [6] guaranties the existence of a function G (such that $\omega = G(Y)$) that is differentiable with respect to $Y(x)$ and whose derivative is:

$$G'(Y) = \left(\frac{\partial^2\varepsilon^2}{\partial\omega_i\partial\omega_j}\right)^{-1}_{(i,j)\in I^2} \times \left(\frac{\partial^2\varepsilon^2}{\partial\omega_i\partial Y_j}\right)_{(i,j)\in I\times J} \tag{9}$$

where I is the set $\{1...n\}$, J the set $\{1...N\}$, n the number of model parameters and N the number of data $Y(x)$.

In our case, we can assume that the additive noise on Y is gaussian, zero mean, spatially uncorrelated and stationary ($\sim N_N\left(0, \Sigma_b = \sigma^2 \times I_N\right)$) so, the differential expression $d\omega = G'(Y)dY$ allows us to compute the covariance matrix of ω:

$$\Sigma_\omega = G'(Y) \times \Sigma_b \times G'(Y)^t \tag{10}$$

So as to compare the precision on interfaces obtained with the present model-based approach and the classical approach (generalized inversion followed by contour extraction), we have also established the law of positions for this latter. This work is developped in an internal document whose main results are given here. To illustrate these results we generate our data by projection of the model given on figure 1.

So as to compare the two reconstructions (from model-based and classical approaches) when the projections are noisy, we add a realistic gaussian noise of standard deviation 8, as presented on figure 2. The comparison of the reconstructions with fitting and generalized inversion are then illustrated on figure 3.

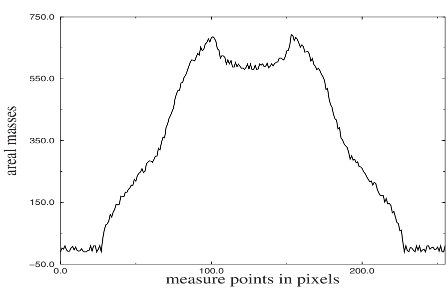

Fig. 2. noisy projection of the model

The strong unstability of the reconstruction obtained by generalized inversion (dotted lines) appears clearly whereas the model obtained by fitting (continuous line) is very similar to figure 1. For fitting, the parameter standard deviations (calculated with formula 10) are very low. We deduce absolute errors less than 2% for densities d_i, and the variation of the interfaces positions does not exceed

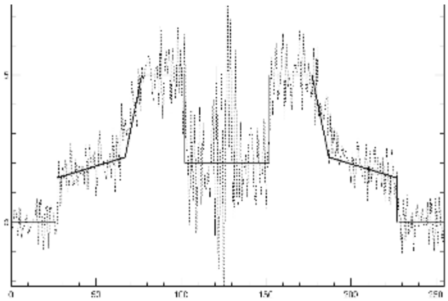

Fig. 3. comparison of the reconstructions (Generalized inversion in dotted and our approach in continuous line)

a half pixel. These results confirm the very good stability of reconstruction by fitting. For generalized inversion, error on density is between 10 and 90% and the standard deviation of interface position error is between 1 and 2 pixels.

We can conclude that ***our approach*** provides undoubtedly a ***very important increase in precision*** on the characteristic parameters that we are looking for.

4 1D Deblurring of 2D Blur

Blur is mainly due to the fact that the X-ray transmitter is not a pinpoint source of light; moreover, the detector acts as a low-pass filter. In the current section, we suppose that the blur kernel H^{2D} associated to those perturbations is circular symmetric with a known shape (from a specific experience). The origin of this perturbation is in the energy domain of X photons (i.e. attenuations of X photons going through the object). So, the blurred projection $\mathcal{Y}_{blur}$ is a function of the ideal projection $\mathcal{Y}$ of the object and is defined by:

$$\mathcal{Y}_{blur}(x,z) = -\left(\frac{\mu}{\rho}\right)^{-1} \ln\left[e^{-\frac{\mu}{\rho}\mathcal{Y}} \underset{x,z}{\star} H^{2D}\right](x,z) \tag{11}$$

This expression allows us to state a very important result: the total mass of the blurred object (M_{blur}) is different from its real mass (M). This is due to the fact that:

$$\left[M_{blur} = \int_{\mathbb{R}^2} \mathcal{Y}_{blur}\right] \neq \left[M = \int_{\mathbb{R}^2} \mathcal{Y}\right] \tag{12}$$

and therefore M can't be deduced directly from the data $\mathcal{Y}_{blur}$.

Mass retrieval of each materials constituting the object is one of the most important goal of our study. So the necessity to deblur the projections $\mathcal{Y}_{blur}$ is evident. Classical operations like Wiener, RIF filtering, ... [17] do not provide satisfactory results in our context because Y exhibits very high frequencies, additive noise is quite white and blur kernels are quite narrow.

In this section, we first deal with the general problem of the deblurring/ reconstruction in one dimension from a projection Y_{blur} blurred with a kernel H (formula 11 written in 1D). Afterwards, we develop the case of two kinds of 3D objects for which this process is achievable.

4.1 The Problem in One Dimension

So as to introduce a deblurring operation during reconstruction by fitting, we define the criteria in the following way:

$$\varepsilon^2 = \sum_{x \in \mathcal{D}} \left[\left(\frac{\mu}{\rho} \right)^{-1} \times \ln \left(e^{-\frac{\mu}{\rho} proj_\omega} \underset{x}{\star} H(x) \right) + Y(x) \right]^2 \tag{13}$$

In order to use a gradient descent to compute the solution of our problem, we first need to verify the differentiability of ε^2 with respect to ω, and so to analyse its partial derivatives with respect to ω_i:

$$\frac{\partial \varepsilon^2}{\partial \omega_i} =$$

$$2 \times \sum_{x \in \mathcal{D}} \left\{ \left[\left(\frac{\mu}{\rho} \right)^{-1} . \ln \left(e^{-\frac{\mu}{\rho} proj_\omega} \underset{x}{\star} H(x) \right) + Y(x) \right] \times \left[\frac{\left(\frac{\partial proj_\omega}{\partial \omega_i} . e^{-\frac{\mu}{\rho} proj_\omega} \right) \underset{x}{\star} H(x)}{e^{-\frac{\mu}{\rho} proj_\omega} \underset{x}{\star} H(x)} \right] \right\} \tag{14}$$

If we denote att_{blur} the blurred attenuation of the object given by:

$$att_{blur}(x) = \int_{I\!R} \left(e^{-\frac{\mu}{\rho} proj_\omega(\tau)} \times H(x-\tau) d\tau \right) \tag{15}$$

then the only problematic term in the computation of the gradient is:

$$\left(\frac{\partial att_{blur}}{\partial \omega_i} \right)(x) = \left(\left(\frac{\partial proj_\omega}{\partial \omega_i} \right) e^{-\frac{\mu}{\rho} proj_\omega} \right) \underset{x}{\star} H(x) \tag{16}$$

because the derivatives of the projection do not exist for all the values of the parameter ω. We have shown that, in fact, the main difficulty is generically reduced to the case of a model with a constant density area whose parameters are called r and D, for which the expression of the previous equation turns out to be:

$$\begin{aligned} \frac{\partial att_{blur}}{\partial r}(x) &= 2.D.r \int_{-r}^{r} \left(\frac{1}{\sqrt{r^2 - \tau^2}} \times e^{-\frac{\mu}{\rho} proj_\omega(\tau)} \times H(x-\tau) d\tau \right) \\ &= \int_{-r}^{r} K(r, \tau, x) d\tau \end{aligned} \tag{17}$$

The function $K(., \tau, .)$ can be integrated on $[-r, r]$ so this expression shows that ε^2 is differentiable if the convolution integral is performed on a continuous domain. In conclusion, the criteria is numerically not differentiable with respect to the r_i.

In the two following items, we demonstrate that, from the definition of a non differentiable criteria, we can supply very good approximations of its "true" gradient (i.e. calculated continuously as in 17) and so ensure the convergence of the minimization scheme to the exact solution.

Explicit Computation of the Gradient. If we denote τ_0 a positive integer lower than r and belonging to the set $\mathcal{D}$ (the set of points of measure x defined in 2.2), then a reformulation of equation 17 leads to:

$$\frac{1}{2.D.r}.\frac{\partial att_{blur}}{\partial r}(x) = \underbrace{\int_{-\tau_0}^{\tau_0} K(r,\tau,x)d\tau}_{\substack{\text{computation by Discrete}\\ \text{Fourier Transform}}} + \underbrace{\int_{\tau_0}^{r} K(r,\tau,x)d\tau}_{\text{first rest } R_1(x)} + \underbrace{\int_{-r}^{-\tau_0} K(r,\tau,x)d\tau}_{R_2(x)=R_1(-x)}$$

The first term is easily computable and the only difficult issue is the rest $R_1(x)$. Thanks to an integration of $R_1(x)$ by parts, we finally get a numerically convergent integral and then the searched approximation of the gradient.

The main drawback of this method is that we must have a formal expression of the blur kernel H, which is not the case in general.

Computation in the Fourier Domain. Let's recall the main problem in equation 16: the generic expression $\frac{\partial proj_\omega}{\partial r}(x)$ does not exist for all x. But, its Fourier Transform is defined everywhere and is given by its cosine transform:

$$\frac{\widehat{\partial proj_\omega}}{\partial r}(f) = \int_{-r}^{r} \frac{1}{\sqrt{r^2-x^2}} \times cos(2\pi x f)dx = \int_0^\pi cos(2\pi r f cos(\theta))d\theta = \pi \times J_0(2\pi r f)$$

We can now write the computation of blurred attenuation (eq. 17) if we adopt the following process:

$$\begin{cases} \frac{\partial att_{blur}}{\partial r}(x) = \left(\frac{\partial proj_\omega}{\partial r} \times e^{-\frac{\mu}{\rho}proj_\omega}\right) \star H(x) \\ \qquad\qquad FT\downarrow \qquad DFT\downarrow \qquad \downarrow DFT \\ \frac{\widehat{\partial att_{blur}}}{\partial r}(f) = \left(\frac{\widehat{\partial proj_\omega}}{\partial r} \star \widehat{e^{-\frac{\mu}{\rho}proj_\omega}}\right) \times \widehat{H}(f) \end{cases} \tag{18}$$

where the convolution, in the Fourier domain, between $\widehat{e^{-\frac{\mu}{\rho}proj_\omega}}$ and $\frac{\widehat{\partial proj_\omega}}{\partial r}$ uses a sampling of $\frac{\widehat{\partial proj_\omega}}{\partial r}$; $\frac{\partial att_{blur}}{\partial r}$ is given by the inverse DFT of $\frac{\widehat{\partial att_{blur}}}{\partial r}$, which finally allows us to provide an approximation of the gradient of ε^2.

If we compare this technique with the one presented previously, we can notice that we don't have to know continuously the blur kernel H. The only constraints come from the sampling of the Fourier Transform of $\frac{\partial proj_\omega}{\partial r}$. It is indeed vanishing very slowly, so the cancellation of high frequencies generates small artefacts. However, these perturbations remain low enough not to disturb the minimization process. This approach is moreover the fastest one.

In the following two subsections, we deal with two kinds of 3D objects for which an extension of 1D deblurring/reconstruction by fitting is possible and moreover, once again, exact.

4.2 Application to "3D Cylindrical Objects"

For this kind of object, the projections $\mathcal{Y}$ are independent of z, so we can identify the 1D projection $Y(x)$ to $\mathcal{Y}(x,z)\,,\forall z$. So as to be able to use the previous results, we must search an expression relating the kernel H^{2D} applied to $\mathcal{Y}$ to a 1D kernel denoted H (that will be convolved with Y) that verifies:

$$\mathcal{Y}_{blur}(x,z) = \mathcal{Y} \underset{x,z}{\star} H^{2D}(x,z) = Y \underset{x}{\star} H(x)\,,\forall z \tag{19}$$

This kernel H is known to be the Abel Transform [3] of H^{2D} and is given by:

$$H(x) = \int_x^{\infty} \left(\frac{2y \times \widetilde{H^{2D}}(y)}{\sqrt{y^2 - x^2}} \right) dy = AT\left[H^{2D}\right](x) \tag{20}$$

with $\widetilde{H^{2D}}(\sqrt{u^2+v^2}) = H^{2D}(u,v),\ \forall (u,v) \in \mathbb{R}^2$.

With this new definition of the criteria to be minimized:

$$\varepsilon^2 = \sum_{x\in\mathcal{D}} \left[\left(\frac{\mu}{\rho}\right)^{-1} \ln\left(e^{-\frac{\mu}{\rho}proj_\omega} \underset{x}{\star} \underbrace{AT\left[H^{2D}\right](x)}_{H} \right) + \mathcal{Y}_{blur}(x,.) \right]^2 \tag{21}$$

the problem is then well posed.

The results we have obtained with this technique are flagrant because, if the blur kernel is known, the reconstruction by model fitting is then exact, whereas classical techniques provide a very smooth reconstruction, often far from the object. An example is illustrated on next figure where our exact reconstruction is drawn in continuous lines and the reconstruction obtained by generalized inversion is in dotted.

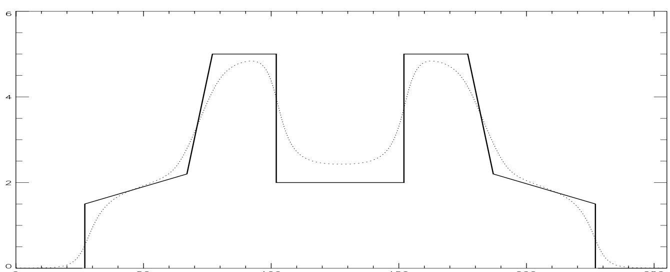

4.3 Application to 3D Spherical Objects

In this case, the 2D data $\mathcal{Y}$ are the projections of a spherical axisymmetrical object. They are then circular symmetrical, centered at the point (c,c) and Y can be defined by $\mathcal{Y}(x,c)$. If we use here a property of the Hankel Transform [3] (denoted HT), we get:

$$HT\left[\mathcal{Y}_{blur}(.,c)\right](q) = HT\left[\mathcal{Y} \underset{x,z}{\star} H^{2D}(.,c)\right](q) = HT[Y](q) \times HT\left[\widetilde{H^{2D}}\right](q) \tag{22}$$

where $\widetilde{H^{2D}}$ is given by formula 4.2. This expression allows us to identify H:

$$HT\left[H\right](q) = HT\left[\widetilde{H^{2D}}\right](q) \tag{23}$$

The problem is then well posed if we formulate the criteria ε^2 as

$$\varepsilon^2 = \sum_{x \in \mathcal{D}} \left[-\left(\frac{\mu}{\rho}\right)^{-1} \ln\left\{ HT^{-1}\left(HT\left[e^{-\frac{\mu}{\rho} proj_\omega}\right] \times HT\left[\widetilde{H^{2D}}\right]\right)(x)\right\} - \mathcal{Y}_{blur}(x, c) \right]^2$$

We demonstrate, thanks to relation 4.3, that the reconstruction is indeed achievable. But the processing of direct and inverse Hankel Transforms remains a delicate problem and extensively increases computation time.

5 Conclusion

In this paper, we have presented an original approach to the problem of tomographic reconstruction of an axisymmetrical object from one view. First, we have developped a 1D study where we deform a simple model of the object based on a description in density areas. We have described the formal aspects of the reconstruction and proposed two efficient regularizations allowing to minimize the derived energy by gradient descent under inequality constraints. We have also studied the bias generated by the noise on projections ; moreover, we have proposed a new formulation of the problem that enables us to deblur the projections during the reconstruction by fitting. In each case, we have compared our results to a reconstruction with generalized inversion ; we have obtained an important improvement in precision on the characteristic parameters we are looking for.

Our future works deal with the warping of a fully 3D axisymmetrical model of the objects. We are now working on the construction of smooth 3D density fields inserted between axisymmetrical surfaces under hypotheses of quasi linearity of the density.

References

1. N. H. Abel. Résolution d'un problème de mécanique. *J. Reine u. Angew. Math.*, 1:153–157, 1826.
2. J. Besag. On the statistical analysis of dirty pictures. *J.R. Static. Soc. Ser. B48*, 3:259–279, 1986.
3. R. Bracewell. *The fourier transform and its applications.* Mc Graw-Hill, , deuxième edition, 1978.
4. J. C. Culioli and P. Charpentier. *cours de l'école nationale des Mines de Paris*, volume II- optimisation libre en dimension finie. 1990.
5. M. Deutsch and I. Beniaminy. Derivative free inversion of abel's integral equation. *Applied Physics Letters*, 41(1), July 1982.
6. J. Dieudonne. *Eléments d'analyse*, volume 3. Gauthier-Villars, 1982.

7. J. M. Dinten. *Tomographie à partir d'un nombre limité de projections: régularisation par des champs markoviens.* PhD thesis, Université de Paris Sud, centre d'Orsay, 1990.
8. A. M. Djafari. Image reconstruction of a compact object from a few number of projections. *IASTED SIP 96, Floride*, November 1996.
9. A. M. Djafari. Slope reconstruction in X-ray tomography. *Processing of SPIE 1997, San Diego*, July 1997.
10. N. J. Dusaussoy. Image reconstruction from projections. *SPIE's international symposium on optics, imaging and instrumentation, San Diego*, July 1994.
11. E. Fugelso. Material density measurement from dynamic flash X-ray photographs using axisymmetric tomography. *Los Alamos Publication*, March 1981.
12. S. Geman and D. Geman. Stochastic relaxation, Gibbs distribution, and the bayesian restoration of images. *Transactions on pattern analysis and machine intelligence*, PAMI 6, n. 6:721–741, 1994.
13. J. Hadamard. Sur les problèmes aux dérivées partielles et leur signification physique. *Princetown University Bulletin*, 1902.
14. K. M. Hanson. Tomographic reconstruction of axially symmetric objects from a single radiograph. *Proceedings of the* 16^{th} *International congress on high speed photography and photonics, Strasbourg*, Août 1984.
15. K. M. Hanson, G. S. Cunningham, G. R. Jennings, and D. R. Wolf. Tomographic reconstruction based on flexible geometric models. *Proceedings of the IEEE international conference on image processing, Austin , Texas*, November 1994.
16. Gabor T. Herman. *Image reconstruction from projections, the fundamentals of computerized tomography.* Academic Press, 1980.
17. A. J. Kain. *Fundamentals of digital signal processing.* Prentice Hall. International edition.
18. J. M. Lagrange. *Reconstruction tomographique à partir d'un petit nombre de vues.* PhD thesis, Ecole Normale Supérieure de Cachan, 1998.
19. H. Maître, C. Pellot, A. Herment, M. Sigelle, P. Horain, and P. Peronneau. A 3D reconstruction of vascular structures from two X-rays angiograms using an adapted simulated annealing algorithm. *IEEE transactions on medical imaging*, 13(1), March 1994.
20. C. Pellot, A. Herment, M. Sigelle, P. Horain, and P. Peronneau. Segmentation, modelling and reconstruction of arterial bifurcations in digital angiography. *Medical and biological engeeneering andcomputing*, November 1992.
21. M. J. D. Powell and Y. Yuan. A recursive quadratic programming algorithm that uses differentiable exact penalty functions. *Mathematical programming*, 35:265–278, 1986.
22. K. Schittkowski. Solving non linear problems with very many constraints. *Optimization*, 25:179–196, 1992.
23. M. Senasli, L. Garnero, A. Herment, and C. Pellot. Stochastic active contour model for 3D reconstruction from two X-ray projections. *1995 international meeting on fully 3D image reconstruction in radiology and nuclear medecine, Grenoble*, July 1995.
24. A. Tikhonov and V. Arsenin. *Solutions off il-posed problems.* Washington DC: Winston, 1977.